Modelling functionalized drug release for a spherical capsule

Elliot J. Carr [a],*, Giuseppe Pontrelli [b]

[a] *School of Mathematical Sciences, Queensland University of Technology (QUT), Brisbane, Australia*
[b] *Istituto per le Applicazioni del Calcolo - CNR, Rome, Italy*

ARTICLE INFO

ABSTRACT

Advances in material design have led to the rapid development of novel materials with increasing complexity and functions in bioengineering. In particular, functionally graded materials (FGMs) offer important advantages in various fields of application. In this work, we consider a heterogeneous reaction-diffusion model for an FGM spherical drug release system that generalizes the multi-layer configuration to arbitrary spatially-variable coefficients. Our model proposes a possible form for the drug diffusivity and reaction rate functions exhibiting fixed average material properties and a drug release profile that can be continuously varied between the limiting cases of a homogeneous system (constant coefficients) and two-layer system (stepwise coefficients). A semi-analytical solution is then used to solve the model, which provides closed-form expressions for the drug concentration and drug release profiles in terms of generalized Fourier series. Our results show how the release rate of the proposed FGM drug release system can be controlled and continuously varied between a fast (homogeneous) and slow (two-layer) release while maintaining the same averaged values for the diffusivity and reaction rate.

1. Introduction

Spherical drug carriers are among the most common formulations for a controlled release system. In particular, microcapsules are small spherical particles produced by coating templates constituted of different polymers and using various fabrication strategies [1]. Although they can be made of a variety of sizes and materials, capsules of interest for most bio-applications have diameters ranging from some nanometers to a few micrometers. Specific examples include liposomes, pellets, nanocontainers, and others [2]. The effectiveness of polymeric delivery systems can be improved by designing structures with modified material properties that are capable of responding to specific pre-set conditions that prescribe the release of the loaded drug.

One of the approaches generally recognized as effective in the assembly of polymer particles is the layer-by-layer technique. These drug carriers are considered as challenging releasing devices because of their unique multi-layer structural properties [3]. Another family of drug delivery systems is constituted by stimuli-responsive capsules that control the release of the therapeutic active agents in response to external triggers such as temperature, pH and many others [4,5]. Among other concurrent effects, such as dissolution, polymer swelling and possible degradation, diffusion remains the most important mechanism used to control the release rate from drug delivery systems [6,7]. Some experiments, however, show that a fraction of the initial drug loaded is retained within the shell and is never released, due to the specific capacity of the polymer to permanently bind the drug molecules [8]. It is common to model this observed phenomenon through first order reaction kinetics [4,8].

Mathematical models of drug release from spherical carriers provide insights of mass transport and drug kinetics involved in drug delivery as well as the effect of design parameters, such as the device geometry and drug loading distribution, on the release mechanism and can significantly reduce the number of experimental studies [9]. However, these models depend on so many variables and parameters that, if not appropriately simplified, can raise more questions than useful answers. Analysis of diffusion-controlled system are confined to homogeneous spheres where an exact solution is available [10], or to layered capsules [11,12], where various mathematical models have been proposed to describe the drug release from this system over the years [1,6,9,15,16].

While such configurations are well understood, there is still room for improvement in mechanistic models to control the release mechanism from a drug-loaded sphere. For example, the effect of non-homogeneity represents an important feature that can influence greatly the release properties. Functionally graded materials (FGMs) are a variety of com-

---

* Corresponding author.
E-mail address: elliot.carr@qut.edu.au (E.J. Carr).
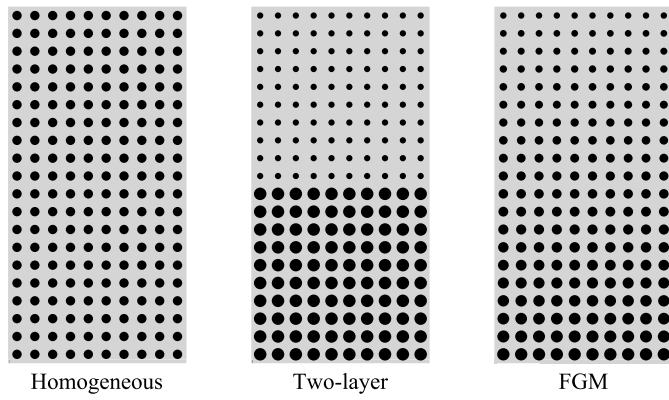
Fig. 1. Schematic representation of an FGM with continuous variation of porosity/density compared to an homogeneous material (no variation) and a two-layer material (stepwise variation).

posite materials in which the material properties vary smoothly and continuously (Fig. 1). This is in contrast to previous approaches for achieving varying material properties, such as layer-by-layer assembly, where there is an abrupt change in properties from one layer to the next. FGMs, i.e composite materials that have a progressive compositional gradient, are already currently used in a wide range of applications [17,18]. Using today's micro-engineering potential, it is possible to manufacture and control the material properties of the substrate to have the desired smart release properties [2]. For example, new possibilities are derived from 3D printing technology to manufacture material micro-porosity and density in non-homogeneous PLGA substrates [19–22].

A mathematical model of drug release from a thin film FGM has been recently presented and solved numerically [23]. In the current work, we propose a reaction-diffusion continuum model to describe drug transport within, and release from, a drug-loaded FGM spherical capsule and develop a semi-analytical eigenfunction expansion solution [24–28] to handle the spatially-variable coefficients. Our model suggests a possible form for the drug diffusivity and reaction rate functions, which exhibits the same average material properties and can be continuously varied between the limiting cases of a homogeneous system (constant coefficients) and two-layer system (stepwise coefficients)

The rest of the article is organized as follows. In the next section, we present the model equations and boundary conditions that govern the drug mass release from a non-homogeneous FGM spherical system. In section 3, we present the semi-analytical solution methodology leading to a closed-form solution. In section 4, drug concentration and drug release profiles are presented for two distinct cases: pure diffusion and reaction-diffusion. Through extensive simulations, we explore the effect of FGM systems on the drug release mechanism by comparing the release profiles to those obtained from standard homogeneous and two-layer systems. Finally, section 5 provides general conclusions and some perspectives for future studies.

2. Using FGM in releasing spherical particles

Drug nanocontainers and releasing microcapsules are the subject of considerable research effort because of their structural and morphological properties, allowing the synthesis of materials capable of responding to biochemical alterations of the environment [4]. Particularly, layer-by-layer polymeric releasing particles have gained increasing interest for their ability to control and tune the release of one or more therapeutic drugs [29]. Here, the layers are constituted of different materials having specific physico-chemical characteristics and are customized to allow a selective diffusion and better control the transfer rate [1]. In the layer-by-layer configuration, a semi-permeable external shell (coating) is often designed to shield and preserve the encapsulated drug from

degradation and chemical aggression, and guarantee a more controlled and sustained release [30]. With the aim of overcoming and generalizing the layered structure, we explore the potential of a material with continuously changing properties.

Recently, more attention has been paid to the class of functionally graded materials (FGMs), in several fields of application [18]. FGMs are a special kind of composite materials in which the microstructural properties vary smoothly and continuously in space [17]. In a purely diffusive model, the continuously varying nature of FGMs naturally lends itself to different functional forms of the diffusion coefficient $D(\mathbf{x})$ in the domain Ω:

$$\frac{\partial c}{\partial t} = \nabla \cdot (D(\mathbf{x})\nabla c), \qquad \mathbf{x} \in \Omega, \quad t \in [0, T], \tag{2.1}$$

where $c(\mathbf{x}, t)$ is the mass volume-averaged concentration of drug. We assume the diffusivity is higher at lower polymer density (inner region) and lower at higher polymer density (outer region), to account for a material that gradually thickens outwards.

From experiments, however, it is observed that a fraction of the initial loaded drug is retained and never released. A possible explanation of this phenomenon is a chemical reaction due to polymer-drug interaction. In other words, due to long polymeric chains and possible electrostatic interactions, a small percentage of the initial loaded drug is entrapped without being released [4]. We model this phenomenon by using reaction kinetics, where the drug molecules travelling through the polymer can potentially be permanently bound with a rate $k(\mathbf{x})$ [8]. This generalizes equation (2.1) to include a first-order reaction term:

$$\frac{\partial c}{\partial t} = \nabla \cdot (D(\mathbf{x})\nabla c) - k(\mathbf{x})c, \qquad \mathbf{x} \in \Omega, \quad t \in [0, T], \tag{2.2}$$

where $k(\mathbf{x})$ $[s^{-1}]$ is a space-dependent reaction rate.

Drug release from an FGM sphere

We consider a reservoir-type drug carrier with an active agent loaded in a spherical polymeric matrix, which is one of the most common formulations for a controlled release system. The spherical carrier is assumed to have radius R giving domain $\Omega = \{\mathbf{x} \in \mathbb{R}^3 \mid \|\mathbf{x}\| < R\}$ and boundary $\partial\Omega = \{\mathbf{x} \in \mathbb{R}^3 \mid \|\mathbf{x}\| = R\}$, where $\|\cdot\|$ is the Euclidean norm. The interior of the spherical capsule is made of a non-homogeneous FGM, reflecting a customized composition that allows for selective spatially-dependent diffusion and reaction to better control the drug transfer rate (Fig. 2). The case of a core-shell capsule is also included in this model, through stepwise diffusivity and reaction functions. As for in-vitro experiments, the sphere is immersed in an external ambient medium of a large extent (relative to size of the sphere), taken as semi-infinite.

In the case of an isotropic sphere centred on the origin with a boundary condition on its outer surface, we can assume that net drug diffusion occurs along the radial (r) direction only, and thus we restrict our study to a one-dimensional model, as follows:

$$\frac{\partial c}{\partial t} = \frac{1}{r^2} \frac{\partial}{\partial r} \left(r^2 D(r) \frac{\partial c}{\partial r} \right) - k(r)c, \qquad r \in [0, R], \quad t \in [0, T], \tag{2.3}$$

$$c(r, 0) = c_0(r), \qquad r \in [0, R], \tag{2.4}$$

$$\frac{\partial c}{\partial r}(0, t) = 0, \qquad t \in [0, T], \tag{2.5}$$

$$-D(R)\frac{\partial c}{\partial r}(R, t) = P\,c(R, t), \qquad t \in [0, T]. \tag{2.6}$$

The model permits a space dependent initial concentration (2.4) and accounts for a flux resistance (with mass transfer coefficient P) at the external surface (2.6) due to the semi-permeable coating [12]. The diffusion model is valid under the usual continuum limit assumptions i.e., drug molecules are small relative to the size of the capsule and move according to a unbiased random walk with spatial and temporal steps that are small relative to the capsule size and release time, respectively.
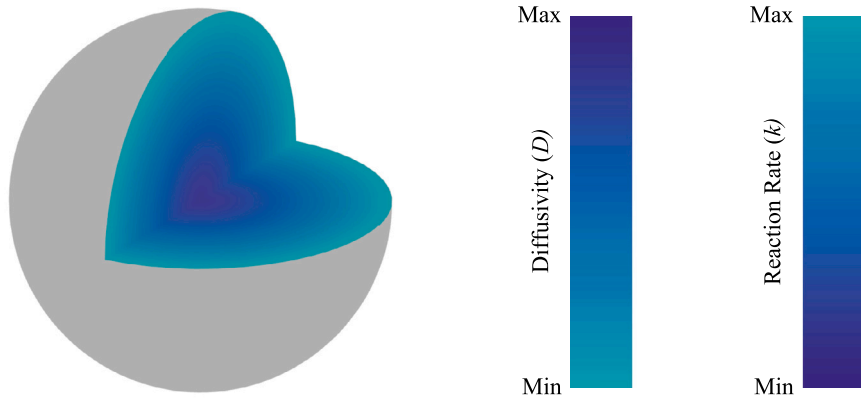
Fig. 2. Schematic diagram of an FGM spherical capsule [20], where the diffusivity varies from a maximum value at the centre to a minimum value at the surface and the reaction rate follows an opposite trend (cf. section 2). (For interpretation of the colours in the figure(s), the reader is referred to the web version of this article.)

α [non dim.]	0.0001	20	80	10000
σ [non dim.]	$-2.414 \cdot 10^4$	$4.330 \cdot 10^{-1}$	$4.839 \cdot 10^{-1}$	$4.997 \cdot 10^{-1}$
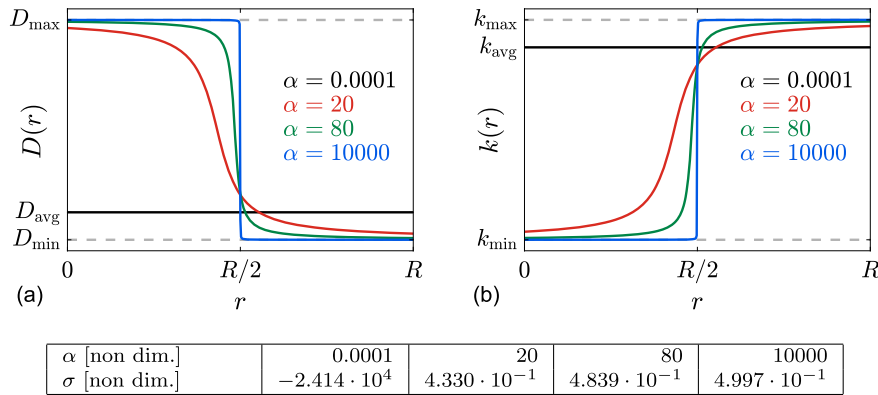
Fig. 3. (a) Diffusivity functions $D(r)$ (2.7) used for both the *pure diffusion* and *reaction-diffusion* cases. (b) Reaction rate functions $k(r)$ (2.11) used for the *reaction-diffusion* case. For each value of α, the table gives the corresponding value of σ satisfying equation (2.10). The combination of a small value of α with a specific large negative value of σ ensures that $D(r)$ is effectively constant and equal to D_{avg} across the interval $0 < r < R$.

The choice of $D(r)$ and $k(r)$

A specific form for $D(r)$ is needed to characterize the material heterogeneity of the FGM. In particular, we assume that the physical medium properties (density or porosity) may change continuously along the radius, being softer in the core and harder towards the surface, leading to a decreasing function $D(r)$ (cf. Fig. 2) that varies from a maximum possible value of D_{max} at the center ($r = 0$) to a minimum possible value of D_{min} at the surface ($r = R$). Among a variety of feasible continuous diffusivity functions, we consider

$$D(r) = D_{\text{max}} + (D_{\text{min}} - D_{\text{max}})\left[\frac{1}{2} + \frac{1}{\pi}\arctan\left(\frac{\alpha(r-\sigma)}{R}\right)\right]. \qquad (2.7)$$

This choice is a standard smooth approximation to a two-layer stepwise diffusivity $D(r) = D_{\text{max}} + (D_{\text{min}} - D_{\text{max}})H(r - \sigma)$ where $H(\cdot)$ is the Heaviside function at $r = \sigma$, with $\alpha > 0$ [–] inversely related to the width of the transition layer and σ [cm] denoting the location of the transition centre (see Fig. 3).

Our aim is to understand the effect of varying α and σ on the drug release profile. For a fair comparison, the same average diffusive properties in all cases is maintained: for a specified choice of α, we compute the corresponding value of σ so that the average value of $D(r)$ over the spherical capsule is constant:

$$\frac{1}{V(\Omega)}\iiint_\Omega D(\mathbf{x})\,d\mathbf{x} = D_{\text{avg}},$$

which simplifies to

$$\frac{3}{R^3}\int_0^R r^2 D(r)\,dr = D_{\text{avg}}, \qquad (2.8)$$

in spherical coordinates, when using radial symmetry and $V(\Omega) = 4\pi R^3/3$. In our results, we set

$$D_{\text{avg}} = \frac{3}{R^3}\left[\int_0^{R/2} r^2 D_{\text{max}}\,dr + \int_{R/2}^R r^2 D_{\text{min}}\,dr\right] = \frac{1}{8}D_{\text{max}} + \frac{7}{8}D_{\text{min}}, \qquad (2.9)$$

which is the unique value that yields $\sigma \to R/2$ in the limiting case of a two-layer stepwise medium ($\alpha \to \infty$). In summary, for a specified choice of α, we calculate σ by solving the nonlinear equation:

$$\frac{3}{R^3}\int_0^R r^2\left(D_{\text{max}} + (D_{\text{min}} - D_{\text{max}})\left[\frac{1}{2} + \frac{1}{\pi}\arctan\left(\frac{\alpha(r-\sigma)}{R}\right)\right]\right)dr$$
$$= D_{\text{avg}}. \qquad (2.10)$$

This formulation includes the two limiting cases of a homogeneous system ($D(r) = D_{\text{avg}}$) and a two-layer system ($D(r) = D_{\text{max}}$ if $0 < r < R/2$ and D_{min} if $R/2 < r < R$).

As a consequence of the decreasing diffusivity towards the external surface (due to the thickening material) the drug reaction rate $k(r)$, which is typically proportional to the polymer density/porosity, undergoes a similar radial variation as $D(r)$, but in the opposite direction (cf. Fig. 2), resulting in an increasing function from a minimum possible value of k_{min} at the centre ($r = 0$) to a maximum possible value of k_{max} at the surface ($r = R$):

$$k(r) = k_{\min} + (k_{\max} - k_{\min}) \left[\frac{1}{2} + \frac{1}{\pi} \arctan \left(\frac{\alpha(r - \sigma)}{R} \right) \right], \qquad (2.11)$$

where the values of α and σ are the same as those used for $D(r)$. As for $D(r)$, the average value of $k(r)$ over the full spherical capsule is constant:

$$\frac{3}{R^3} \int_0^R r^2 k(r) \, dr = k_{\mathrm{avg}} = \frac{1}{8} k_{\min} + \frac{7}{8} k_{\max}.$$

3. Solution methodology

We solve the heterogeneous reaction-diffusion model (2.3)–(2.6) by introducing the following non-dimensional variables:

$$\hat{r} := \frac{r}{R}, \qquad \hat{t} := \frac{D_{\max} t}{R^2}, \qquad \hat{c}(\hat{r}, \hat{t}) := \frac{c(r,t)}{C_0}, \qquad (3.1)$$

$$\hat{c}_0(\hat{r}) := \frac{c_0(r)}{C_0}, \qquad \hat{T} := \frac{D_{\max} T}{R^2}, \qquad \hat{P} := \frac{PR}{D_{\max}}, \qquad (3.2)$$

$$\hat{D}(\hat{r}) := \frac{D(r)}{D_{\max}}, \qquad \hat{k}(\hat{r}) := \frac{R^2 k(r)}{D_{\max}}, \qquad \hat{\alpha} := \alpha, \qquad \hat{\sigma} := \frac{\sigma}{R}, \qquad (3.3)$$

where $C_0 = \max_{r \in [0,R]} c_0(r)$. This yields a non-dimensional analogue of equations (2.3)–(2.6):

$$\frac{\partial \hat{c}}{\partial \hat{t}} = \frac{1}{\hat{r}^2} \frac{\partial}{\partial \hat{r}} \left(\hat{r}^2 \hat{D}(\hat{r}) \frac{\partial \hat{c}}{\partial \hat{r}} \right) - \hat{k}(\hat{r}) \hat{c}, \qquad \hat{r} \in [0,1], \quad \hat{t} \in [0, \hat{T}], \qquad (3.4)$$

$$\hat{c}(\hat{r}, 0) = \hat{c}_0(\hat{r}), \qquad \hat{r} \in [0, 1], \qquad (3.5)$$

$$\frac{\partial \hat{c}}{\partial \hat{r}}(0, \hat{t}) = 0, \qquad \hat{t} \in [0, \hat{T}], \qquad (3.6)$$

$$-\hat{D}(1) \frac{\partial \hat{c}}{\partial \hat{r}}(1, \hat{t}) = \hat{P} \hat{c}(1, \hat{t}), \qquad \hat{t} \in [0, \hat{T}]. \qquad (3.7)$$

Equations (3.4)–(3.7) constitute a linear problem with spatially-variable coefficients and homogeneous boundary conditions. To solve this problem, we use a semi-analytical approach where $\hat{c}(\hat{r}, \hat{t})$ is expanded in terms of orthonormal eigenfunctions:

$$\hat{c}(\hat{r}, \hat{t}) = \sum_{n=1}^{\infty} T_n(\hat{t}) X_n(\hat{r}), \qquad (3.8)$$

where, due to orthonormality:

$$T_n(\hat{t}) = \int_0^1 \hat{r}^2 \hat{c}(\hat{r}, \hat{t}) X_n(\hat{r}) \, d\hat{r}. \qquad (3.9)$$

In the framework of the Classical/General Integral Transform Technique (CITT/GITT), (3.8) and (3.9) are known as the *inverse transform* and the *integral transform*, respectively [26,27]. Before proceeding further, we note that our solution approach differs to the semi-analytical Laplace transform method used in our previous work [12] for diffusion-controlled release from a multi-layer spherical capsule (without reaction). A short comparison between the two approaches is given in Appendix A.

The space function $X_n(\hat{r})$

In the solution expansion (3.8), we let $X_n(\hat{r})$ be the eigenfunctions associated with the following Sturm-Liouville problem:

$$\frac{1}{\hat{r}^2} \frac{d}{d\hat{r}} \left(\hat{r}^2 \frac{dX}{d\hat{r}} \right) = -\lambda^2 X, \qquad (3.10)$$

$$-\hat{D}(1) \frac{dX}{d\hat{r}}(1) = \hat{P} X(1). \qquad (3.11)$$

Note that this is not the Sturm-Liouville problem obtained by applying separation of variables directly to the governing equations. The simplified Sturm-Liouville problem (3.10)–(3.11), on the other hand, admits simple closed-form solutions, a feature that in our view outweighs any

possible disadvantages such as potentially more terms being required in the infinite series (3.8) to achieve a desired level of convergence. We note that similar approaches using simplified Sturm-Liouville problems have previously been employed to solve a heat conduction problem with spatially-varying coefficients [13,31].

The general solution of equation (3.10) is

$$X(\hat{r}) = \frac{A \sin(\lambda \hat{r})}{\hat{r}} + \frac{B \cos(\lambda \hat{r})}{\hat{r}}. \qquad (3.12)$$

To ensure this solution remains finite as $\hat{r}$ tends to zero, we require $B = 0$. Substituting (3.12) into the boundary condition (3.11) then yields:

$$A \left[(\hat{P} - \hat{D}(1)) \sin(\lambda) + \hat{D}(1) \lambda \cos(\lambda) \right] = 0, \qquad (3.13)$$

which has a non-trivial solution ($A \neq 0$) if and only if λ is a solution of

$$(\hat{P} - \hat{D}(1)) \sin(\lambda) + \hat{D}(1) \lambda \cos(\lambda) = 0, \qquad (3.14)$$

or equivalently:

$$\tan(\lambda) = \frac{\hat{D}(1) \lambda}{\hat{D}(1) - \hat{P}}. \qquad (3.15)$$

The eigenvalues, denoted by λ_n for $n \in \mathbb{N}^+$, are defined as the positive values of λ satisfying (3.15) with the corresponding eigenfunctions given by:

$$X_n(\hat{r}) = \frac{2\sqrt{\lambda_n}}{\sqrt{2\lambda_n - \sin(2\lambda_n)}} \frac{\sin(\lambda_n \hat{r})}{\hat{r}}, \qquad (3.16)$$

which are orthonormal on the interval $[0, 1]$:

$$\int_0^1 \hat{r}^2 X_n(\hat{r}) X_m(\hat{r}) \, d\hat{r} = \begin{cases} 0, & \text{if } m \neq n, \\ 1, & \text{if } m = n. \end{cases} \qquad (3.17)$$

The time function $T_n(\hat{t})$

In the solution expansion (3.8), the time functions $T_n(\hat{t})$ are computed by imposing that (3.8) satisfy the actual governing equation (3.4) with space dependent $\hat{D}(\hat{r})$ and $\hat{k}(\hat{r})$. We first substitute (3.8) into (3.4) and differentiate to give

$$\sum_{n=1}^{\infty} \frac{dT_n}{d\hat{t}} X_n(\hat{r}) = \sum_{n=1}^{\infty} T_n(\hat{t}) \left[\hat{D}'(\hat{r}) X_n'(\hat{r}) + \frac{\hat{D}(\hat{r})}{\hat{r}^2} \frac{d}{d\hat{r}} \left(\hat{r}^2 \frac{dX_n}{d\hat{r}} \right) \right]$$

$$- \hat{k}(\hat{r}) \sum_{n=1}^{\infty} T_n(\hat{t}) X_n(\hat{r}).$$

Next, multiplying both sides of this equation by $\hat{r}^2 X_m(\hat{r})$ and integrating from $\hat{r} = 0$ to $\hat{r} = 1$, we see that $T_m(\hat{t})$ satisfies the following differential equation

$$\frac{dT_m}{d\hat{t}} = \sum_{n=1}^{\infty} T_n(\hat{t}) \left[\int_0^1 \hat{r}^2 \hat{D}'(\hat{r}) X_n'(\hat{r}) X_m(\hat{r}) \, d\hat{r} \right.$$

$$\left. - \int_0^1 \hat{r}^2 (\lambda_n^2 \hat{D}(\hat{r}) + \hat{k}(\hat{r})) X_n(\hat{r}) X_m(\hat{r}) \, d\hat{r} \right]$$

$$= \sum_{n=1}^{\infty} A_{mn} T_n(\hat{t}), \qquad (3.18)$$

after making use of the differential equation (3.10) and orthogonality (3.17). Equation (3.18) identifies

$$A_{mn} = \int_0^1 \hat{r}^2 \hat{D}'(\hat{r}) X_n'(\hat{r}) X_m(\hat{r}) \, d\hat{r} - \int_0^1 \hat{r}^2 \left[\lambda_n^2 \hat{D}(\hat{r}) + \hat{k}(\hat{r}) \right] X_n(\hat{r}) X_m(\hat{r}) \, d\hat{r},$$

$$(3.19)$$

Table 1
Parameters of the problem.

Parameter	Description	Value [dim.]	Value [non dim.]
R	Radius	10^{-4} cm	1
$D_{\min}$	Minimum diffusivity	10^{-13} cm^2/s	10^{-2}
$D_{\max}$	Maximum diffusivity	10^{-11} cm^2/s	1
D_{avg}	Average diffusivity	$1.3375 \cdot 10^{-12}$ cm^2/s	0.13375
$k_{\min}$	Minimum reaction rate	$8 \cdot 10^{-5}$ /s	0.08
$k_{\max}$	Maximum reaction rate	10^{-4} /s	0.1
k_{avg}	Average reaction rate	$9.75 \cdot 10^{-5}$ /s	0.0975
P	Mass transfer coefficient	$5 \cdot 10^{-8}$ cm/s	0.5
T	Maximum time	$3 \cdot 10^4$ s	30
C_0	Initial concentration	0.4 mol/cm^3	1

where $X_n'(\hat{r})$, appearing in the definition of A_{mn} (3.19), is given by:

$$X_n'(\hat{r}) = \frac{2\sqrt{\lambda_n}}{\sqrt{2\lambda_n - \sin(2\lambda_n)}} \left[\frac{\lambda_n \cos(\lambda_n\hat{r})}{\hat{r}} - \frac{\sin(\lambda_n\hat{r})}{\hat{r}^2} \right].$$

The appropriate initial condition for the differential equation (3.18) is identified by combining the initial condition (3.5) with the expansion (3.8)

$$\sum_{n=1}^{\infty} T_n(0) X_n(\hat{r}) = \hat{c}_0(\hat{r}),$$

and then applying orthogonality (3.17):

$$T_n(0) = \int_0^1 \hat{r}^2 \hat{c}_0(\hat{r}) X_n(\hat{r}) \, d\hat{r}. \tag{3.20}$$

Assembling the differential equations (3.18) and initial condition (3.20) for $m \in \mathbb{N}^+$ together yields a system of coupled linear differential equations:

$$\frac{d\mathbf{T}}{d\hat{t}} = \mathbf{A}\mathbf{T}, \quad \mathbf{T}(0) = \mathbf{T}_0, \tag{3.21}$$

where the entries of $\mathbf{A}$ are defined in equation (3.19) and $\mathbf{T}_0 = [T_1(0), T_2(0), \ldots]^T$. The exact solution of (3.21) is expressed in terms of a matrix exponential

$$\mathbf{T}(\hat{t}) = e^{\hat{t}\mathbf{A}} \mathbf{T}_0, \tag{3.22}$$

with the nth entry of $\mathbf{T}(\hat{t})$ defining the time function $T_n(\hat{t})$ in the solution expansion (3.8).

Fraction of drug released

To characterise the release process, we calculate the cumulative fraction of drug released as a function of time, $\hat{M}(t)$. This quantity is obtained by integrating the concentration flux over the outer surface of the spherical capsule and normalizing by the initial mass of drug loaded in the capsule:

$$\hat{M}(t) = \frac{\int_0^t \left[\iint_{\partial\Omega} (-D(\mathbf{x})\nabla c(\mathbf{x}, s) \cdot \mathbf{n}) \, d\mathbf{x} \right] ds}{\iiint_\Omega c_0(\mathbf{x}) \, d\mathbf{x}}, \tag{3.23}$$

where $\mathbf{n}$ is the unit vector normal to $\partial\Omega$ directed outward from Ω. In spherical coordinates under radial symmetry, $\hat{M}(t)$ simplifies to

$$\hat{M}(t) = \frac{R^2 \int_0^t -D(R)\frac{\partial c}{\partial r}(R, s) \, ds}{\int_0^R r^2 c_0(r) \, dr}.$$

Using the boundary condition at the outer surface (2.6) and the dimensionless variables (3.1)–(3.3) yields:

$$\hat{M}(\hat{t}) = \frac{\int_0^{\hat{t}} \hat{P}\hat{c}(1, s) \, ds}{\int_0^1 \hat{r}^2 \hat{c}_0(\hat{r}) \, d\hat{r}}.$$

Finally, inserting the solution expansion (3.8) gives the final form for the fraction of drug released

$$\hat{M}(\hat{t}) = \frac{\hat{P} \sum_{n=1}^{\infty} U_n(\hat{t}) X_n(\hat{r})}{\int_0^1 \hat{r}^2 \hat{c}_0(\hat{r}) \, d\hat{r}}, \tag{3.24}$$

where the nth entry of the vector $\mathbf{U}(\hat{t}) = \int_0^{\hat{t}} \mathbf{T}(s) \, ds = (e^{\hat{t}\mathbf{A}} - \mathbf{I})\mathbf{A}^{-1}\mathbf{T}_0$ defines $U_n(\hat{t}) = \int_0^{\hat{t}} T_n(s) \, ds$.

4. Numerical results

We now present numerical results for two distinct cases: *pure diffusion* ($k(r) = 0$) and *reaction-diffusion* ($k(r) > 0$). All results are calculated using a uniform initial concentration $c_0(r) = C_0$ and the parameter values given in Table 1. We have implemented the analytical solution in MATLAB using a simple bisection method to solve the eigenvalue equation (3.14) and truncating all infinite series at $N = 150$ terms (chosen by repeatedly incrementing N by 10 until no changes in the reported concentration (3.8) and mass (3.24) profiles were visibly perceptible). Discussion on the convergence behaviour of the semi-analytical solution is given in Appendix B. The in-built MATLAB functions integral, expm and fzero are used, respectively, to (i) evaluate the integrals in equations (3.19) and (3.20) (ii) compute the matrix exponential $e^{\hat{t}\mathbf{A}}$ and (iii) solve the nonlinear equation (2.10) for σ. Further implementation details are available in our code, which can be downloaded from https://github.com/elliotcarr/Carr2023a.

We limit our investigation to the diffusivity and reaction rate functions, $D(r)$ and $k(r)$, in equations (2.7) and (2.11) and explore the effect of the parameter α. The value of σ depends on the value of α while the role of the surface mass transfer parameter P is fixed and not investigated here. Four different values of α are chosen giving a variety of different drug release profiles that are compatible with these kind of drug release systems. Fig. 3 displays the diffusivity function $D(r)$ and reaction rate function $k(r)$ for the parameter values in Table 1 and the different choices of α. Observe that the smallest value of α accurately captures the case of a homogeneous medium (e.g. $D(r) = D_{\text{avg}}$), while the largest value of α accurately captures the case of a two-layer medium (e.g. $D(r) = D_{\max}$ if $0 < r < R/2$ and $D(r) = D_{\min}$ if $R/2 < r < R$).
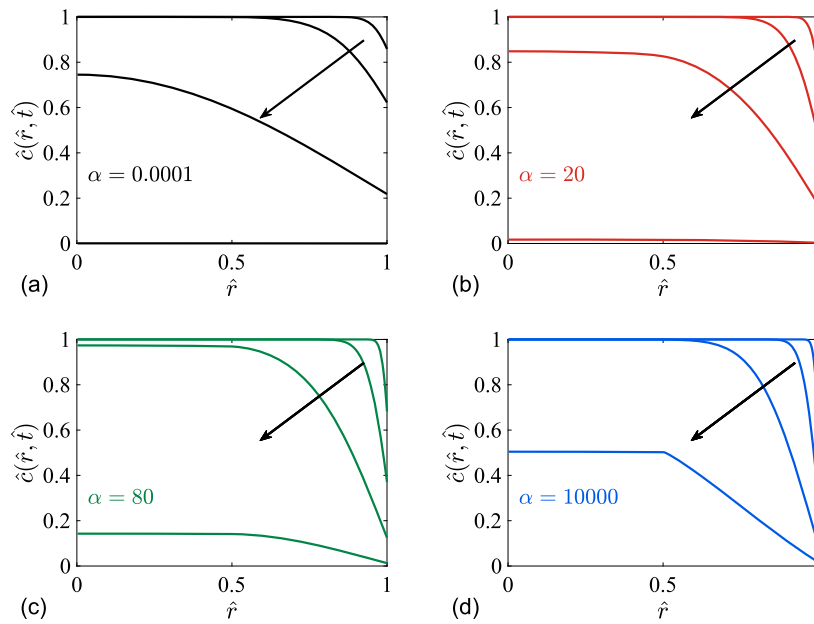
Fig. 4. Drug concentration as a function of radius (3.8) for the *pure diffusion* case. Profiles are shown at four distinct times, $\hat{t} = 10^{-2}, 10^{-1}, 10^{0}, 10^{1}$, with the black arrow indicating the direction of increasing time.
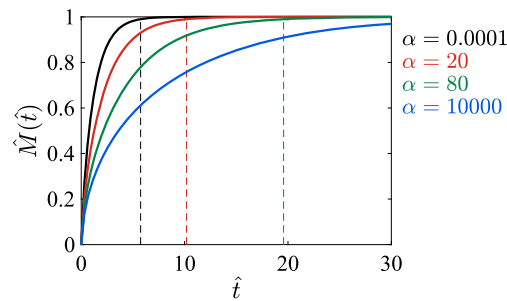
Fig. 5. Cumulative fraction of drug released as a function of time (3.24) for the *pure diffusion* case. Vertical dashed lines indicate approximate release times, $\hat{t}_R$, corresponding to when 99% of the total released mass has been released, i.e. $\hat{M}(\hat{t}_R) = 0.99 \lim_{\hat{t}\to\infty} \hat{M}(\hat{t})$. The release time for $\alpha = 10000$ exceeds 30 and is not shown.

For the case of pure diffusion, drug is retained and released differently depending on the parameter α (Figs. 4, 8 and 9) and these results demonstrate the wide variety of concentration profiles using FGMs. Drug molecules, when travelling from the center to the outer surface, pass through regions where D is progressively reducing. This causes the transport of drug molecules to be hindered by the drug's reduced ability to diffuse and the drug release is slowed down. For $\alpha \to \infty$, steeper concentration gradients are observed at the outer surface ($\hat{r} = 1$).

In Fig. 5, we see that the fraction of drug released increases more rapidly when decreasing the value of α, giving rise to a quicker overall drug delivery for small values of α and a more-sustained release for large values of α. The *initial burst* of dose at small α may be beneficial when a rapid delivery, rather than a delayed sustained release, is desired. Actually, in some circumstances, maintaining local drug concentrations within some defined therapeutic range is desirable, while in other cases a *burst* of drug is required. If the release is not controlled appropriately, this can lead to periods where toxic and/or sub-therapeutic concentrations are achieved. The inclusion of the spatially-varying diffusivity (2.7) provides greater control over the drug release profile (through the single tuning parameter α) while maintaining the same average material properties (2.8).

Let us now consider the reaction-diffusion case. When reaction is included in the model through the function $k(r)$ in eqn. (2.11), the capsule retains a fraction of mass that remains bound to the polymer and is never released. This yields concentration curves (Figs. 6 and 10) that

are lower than the corresponding curves for pure diffusion (Figs. 4 and 9): this is due to the added binding to the polymer region, that becomes stronger towards the surface. When the binding effect is included, more drug is retained within the polymer, yielding a reduced release rate (Figs. 4-7). Since the total released mass is less than the initial mass of drug loaded in the capsule (cf. equation (3.23)), the cumulative fraction of drug released asymptotes to a value less than one (Fig. 7). Comparing the drug release profiles for reaction-diffusion with the corresponding profiles for pure diffusion (Figs. 5 and 7), it is clear that (i) the presence of reaction results in decreased release times and (ii) the total released mass decreases for increasing values of α (Fig. 7). Hence, the inclusion of a functionally-graded reaction in the model provides further control of the drug release profile through the tuning parameter α and reveals novel kinetics with respect to the homogeneous materials.

In summary, our model demonstrates that FGMs are able to provide a variety of drug release characteristics different from those provided by the limiting cases of a homogeneous system (constant coefficients) and two-layer system (stepwise coefficients) while maintaining the same average material properties (same averaged diffusivity and reaction rate). An important question is whether similar release profiles can be achieved using a homogeneous or two-layer capsule. An example of this is presented in Fig. 11, which shows the difference between the release profile for an FGM capsule (pure diffusion case with $\alpha = 80$, i.e., green profile from Fig. 5) and release profiles for best-fit homogeneous and two-layer capsules (see our MATLAB code for full details). This figure
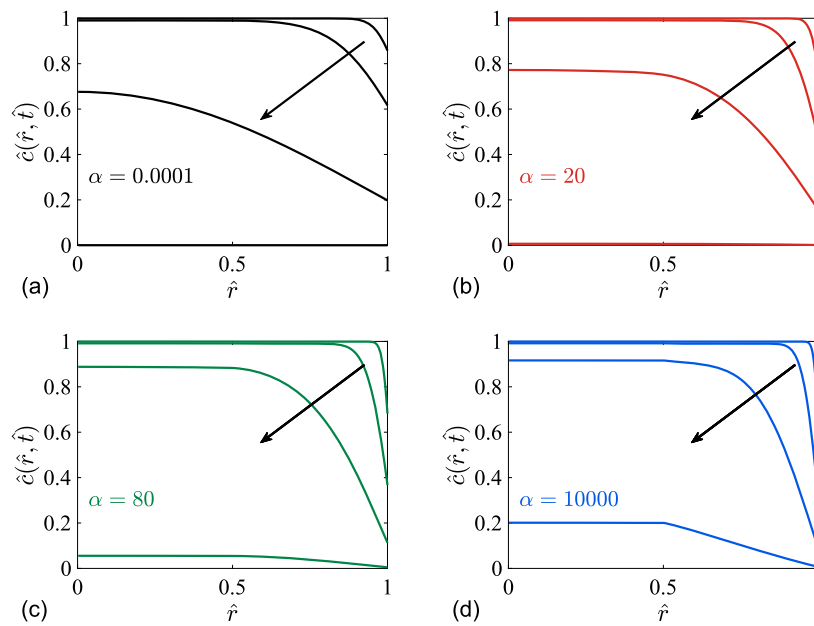
Fig. 6. Drug concentration as a function of radius (3.8) for the *reaction-diffusion* case. Profiles are shown at four distinct times, $\hat{t} = 10^{-2}, 10^{-1}, 10^{0}, 10^{1}$, with the black arrow indicating the direction of increasing time.
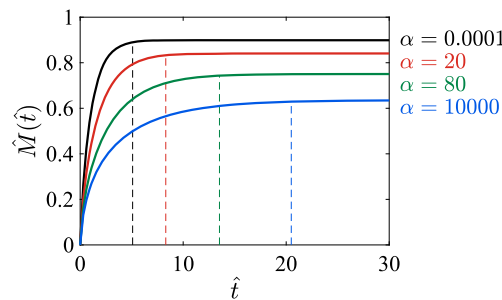
Fig. 7. Cumulative fraction of drug released as a function of time (3.24) for the *reaction-diffusion* case. Vertical dashed lines indicate approximate release times, $\hat{t}_R$, corresponding to when 99% of the total released mass has been released, i.e. $\hat{M}(\hat{t}_R) = 0.99 \lim_{\hat{t} \to \infty} \hat{M}(\hat{t})$.

reveals small differences between the release profiles of approximately 1% and 2% for the two-layer and homogeneous capsules, respectively. While these results demonstrate that precisely the same release profile cannot be achieved using a homogeneous or two-layer capsule, differences of between 1% and 2% probably don't justify using an FGM over traditional homogeneous and two-layer structures. However, it is important to note that this study has focused on the particular diffusivity and reaction rate functions, $D(r)$ and $k(r)$, given in equations (2.7) and (2.11) only. Different choices for $D(r)$ and $k(r)$ may provide release profiles that cannot be well approximated by homogeneous and two-layer capsules. Such analysis requires more extensive investigations, and is left for future work. In practice, the specific form for the FGM material functions should also be tailored according to therapeutic needs, but again this is beyond the scope of the current work.

5. Conclusions

Polymeric engineered materials have been exploited in a range of different application in biomedicine, aerospace and material science and can be useful in the pharmaceutical industry in the field of drug delivery. With recent advances in bioengineering, novel functionally graded materials (FGMs) have been introduced for the development of drug releasing devices and systems. They contribute to the tailoring of material for optimal drug administration including targeted release and customizability.

The goal of the present study was to elucidate the potential transport mechanism and the drug kinetics behaviour due to the diffusion and reaction shape-material functions, providing insight for designing the micro-structure of polymer platforms and capsules. A family of space-dependent sigmoid functions for the diffusivity and reaction rate have been proposed and implemented. Through a sensitivity analysis, the role of the parameter α appearing in the diffusion and reaction rate functions has been demonstrated. The semi-analytical solution improves the understanding of the mass transfer from an FGM capsule, including the presence of a binding reaction. The proposed methodology offers a cheap and useful tool that can be used to quantitatively characterize the drug kinetics, the release time, improve the technological performance and optimize the release rate for the target application.

However, it is important to recognize some limitations of the present one-dimensional model. Drug dynamics in the release medium outside the capsule are ignored, so that the interactions between the capsule and the medium are represented entirely by the boundary condition at the external surface. Diffusion coefficients are also assumed to be independent of concentration. For most practical applications such assumptions are reasonable, and therefore, the model results may be helpful in the evaluation of drug kinetics and may provide new pathways for smarter delivery systems. The strategy proposed here, once calibrated, can be utilized in a predictive way to limit the number of experiments. Thus, by showing the correlation between properties of the drug kinetics and material function variables, our model can be
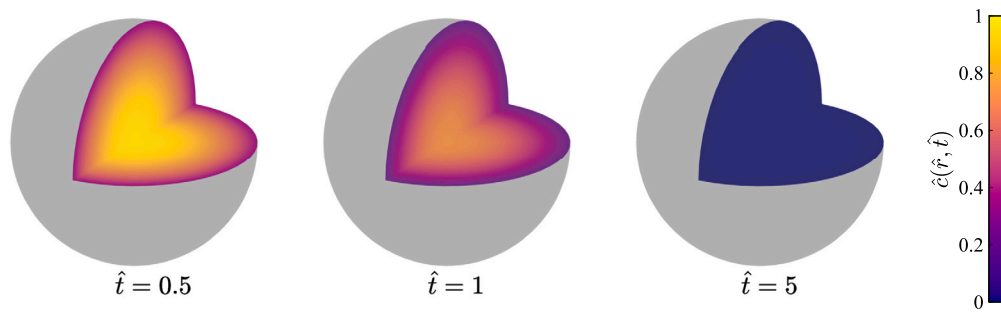
Fig. 8. Drug concentration distribution (3.8) over time for the *pure diffusion case* ($\alpha = 0.0001$).
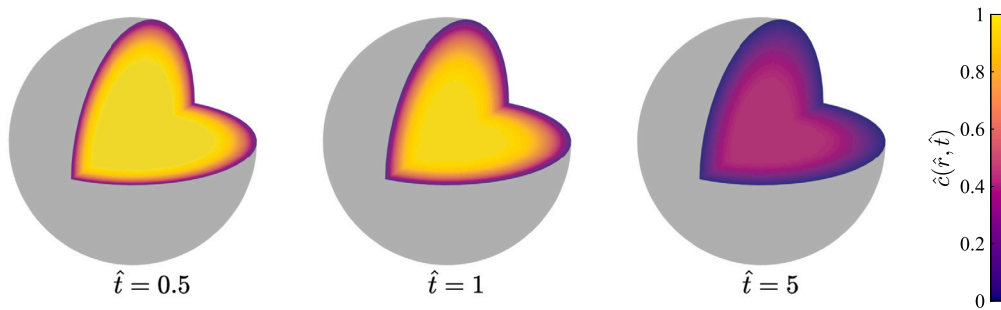
Fig. 9. Drug concentration distribution (3.8) over time for the *pure diffusion case* ($\alpha = 80$).
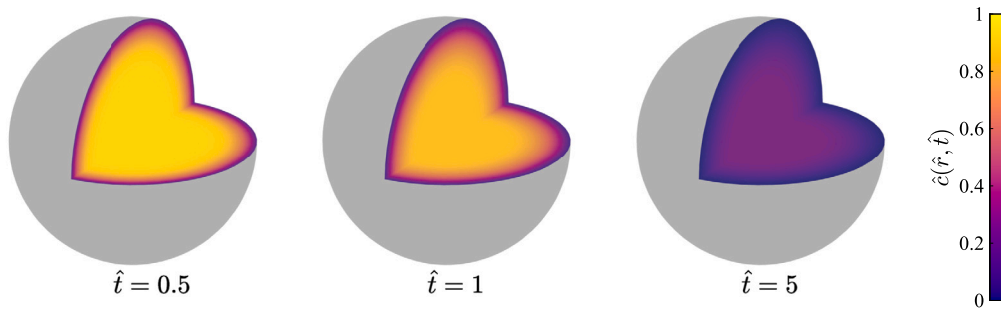
Fig. 10. Drug concentration distribution (3.8) over time for the *reaction diffusion case* ($\alpha = 80$).
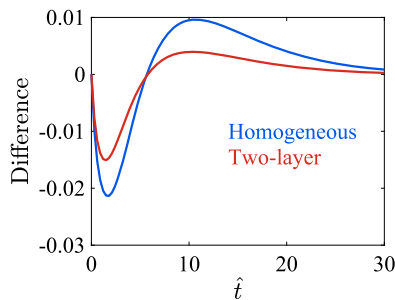
Fig. 11. Difference between the cumulative fraction of drug released as a function of time (3.24) for an FGM capsule (pure diffusion case with $\alpha = 80$, i.e., green profile from Fig. 5) and (i) a homogeneous capsule using a best-fit diffusivity of $D = 2.1875 \cdot 10^{-13}$ (blue curve) (ii) a two-layer capsule using a best-fit diffusivity of $D = 2.0938 \cdot 10^{-13}$ if $0 < r < \sigma$ and $D = 6.5781 \cdot 10^{-12}$ if $\sigma < r < R$ with $\sigma = 5.593 \cdot 10^{-5}$ (red curve). See our MATLAB code for full details. The difference represents the best-fit release profile subtracted from the FGM release profile.

used to determine and optimize the processing parameters to ensure a controlled drug delivery within a certain time.

Finally, by virtue of the one-to-one analogy between mass diffusion and heat conduction problems, the presented FGM approach can be successfully applied to the equivalent model of heat transfer from spheres.

CRediT authorship contribution statement

Elliot J. Carr: Data curation, Formal analysis, Investigation, Methodology, Software, Validation, Visualization, Writing – original draft, Writing – review & editing. **Giuseppe Pontrelli:** Conceptualization, Investigation, Methodology, Writing – original draft, Writing – review & editing.

Declaration of competing interest

The authors declare that they have no known competing financial interests or personal relationships that could have appeared to influence the work reported in this paper.

Data availability

MATLAB code implementing the semi-analytical solution and reproducing the results of the paper is available on GitHub: https://github.com/elliotcarr/Carr2023a.
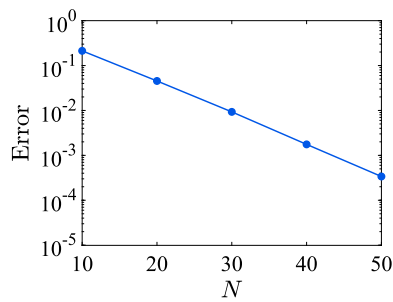
Fig. 12. Error of the semi-analytical solution (section 3) when truncating all infinite series at N terms. The error is calculated as the maximum absolute difference between the semi-analytical solution (3.8) with N terms and a reference solution (semi-analytical solution with 150 terms). Results are given for an FGM capsule (pure diffusion case with $\alpha = 80$, see concentration profiles from Fig. 4(c)) with the maximum absolute difference of the concentration taken over both space $\hat{r} \in (0, 1)$ and time $\hat{t} = 10^{-2}, 10^{-1}, 10^0, 10^1$.

Acknowledgements

Appendix A. Comparison to Laplace transform approach

In previous work [12], we presented a semi-analytical solution based on the Laplace transform for diffusion-controlled release from a multi-layer spherical capsule (without reaction). A similar approach could also be applied to solve the heterogeneous reaction-diffusion model (2.3)–(2.6) considered in the present work. In this case, taking Laplace transforms of the non-dimensional model (3.4)–(3.7) yields a time-independent boundary value problem for the transformed solution $\overline{c}(r, s) = \int_0^\infty e^{-st} c(r, t)\, \mathrm{d}t$. The solution of this boundary value problem in the Laplace domain could then be expanded in terms of the same orthonormal eigenfunctions (3.16), namely $\overline{c}(r, s) = \sum_{n=1}^\infty \alpha_n(s) X_n(\hat{r})$. In this approach, the coefficients $\alpha_n(s)$ ($n = 1, 2, \ldots$) will be identified by solving a system of coupled linear algebraic equations instead of the system of coupled linear differential equations (3.21) required in the current paper. However, after solving this system for the coefficients, the Laplace transform still needs to be inverted to transform $\overline{c}(r, s)$ back to the time domain. Since such an inversion is too difficult to carry out analytically in closed-form (the coefficients will be highly complicated) and numerical inversion can yield unreliable results [14], we have not considered this approach further in the current paper.

Appendix B. Convergence of semi-analytical solution

The semi-analytical solution (section 3) truncates all infinite series at N terms. In this appendix, we briefly explore the convergence behaviour when increasing N for a chosen test problem (pure diffusion case with $\alpha = 80$, see concentration profiles from Fig. 4(c)). For this problem a reference solution was calculated using 150 terms (chosen by repeatedly incrementing N by 10 until the maximum absolute difference, taken over both space $\hat{r} \in (0, 1)$ and time $\hat{t} = 10^{-2}, 10^{-1}, 10^0, 10^1$, between consecutive concentration profiles was less than 10^{-6}). Fig. 12 shows that the error for this problem reduces according to a power law: Error $\propto 10^{-mN}$ for $10 < N < 50$, where m is the slope of the line shown. For the chosen problem, these results also demonstrate that solutions of acceptable accuracy (Error $\sim 10^{-3}$ or 10^{-4}, visibly indiscernible from reference solution) can be obtained using around 40 or 50 terms.

References

[1] A.S. Timin, D.J. Gould, G.B. Sukhorukov, Multi-layer microcapsules: fresh insights and new applications, Expert Opin. Drug Deliv. 14 (5) (2017) 583–587.

[2] S. De Koker, R. Hoogenboom, B.G. De Geest, Polymeric multilayer capsules for drug delivery, Chem. Soc. Rev. 41 (2012) 2867–2884.

[3] M. Matsusaki, M. Akashi, Functional multilayered capsules for targeting and local drug delivery, Expert Opin. Drug Deliv. 6 (2009) 1207–1217.

[4] G. Pontrelli, G. Toniolo, S. McGinty, D. Peri, S. Succi, C. Chatgilialoglu, Mathematical modelling of drug delivery from pH-responsive nanocontainers, Comput. Biol. Med. 131 (2021) 104238.

[5] J. Majumder, T. Minko, Multifunctional and stimuli-responsive nanocarriers for targeted therapeutic delivery, Expert Opin. Drug Deliv. 18 (2021) 205–227.

[6] D.Y. Arifin, L.Y. Lee, C.H. Wang, Mathematical modeling and simulation of drug release from microspheres: implications to drug delivery systems, Adv. Drug Deliv. Rev. 58 (2006) 1274–1325.

[7] M. Grassi, G. Lamberti, S. Cascone, G. Grassi, Mathematical modeling of simultaneous drug release and in vivo absorption, Int. J. Pharm. 418 (2011) 130–141.

[8] E. Barchiesi, T. Wareing, L. Desmond, A.N. Phan, P. Gentile, G. Pontrelli, Characterization of the shells in layer-by-layer nanofunctionalized particles: a computational study, Front. Bioeng. Biotechnol. (2022) 888944.

[9] A. Hadjitheodorou, G. Kalosakas, Analytical and numerical study of diffusion-controlled drug release from composite spherical matrices, Mater. Sci. Eng. C 42 (2014) 681–690.

[10] J. Crank, The Mathematics of Diffusion, Oxford Univ. Press, 1975.

[11] B. Kaoui, M. Lauricella, G. Pontrelli, Mechanistic modelling of drug release from multi-layer capsules, Comput. Biol. Med. 93 (2018) 149–157.

[12] E.J. Carr, G. Pontrelli, Modelling mass diffusion for a multi-layer sphere immersed in a semi-infinite medium: application to drug delivery, Math. Biosci. 303 (2018) 1–9.

[13] E.J. Carr, I.W. Turner, A semi-analytical solution for multilayer diffusion in a composite medium consisting of a large number of layers, Appl. Math. Model. 40 (15–16) (2018) 7034–7050.

[14] E.J. Carr, New semi-analytical solutions for advection-dispersion equations in multilayer porous media, Transp. Porous Media 135 (2020) 39–58.

[15] M.R. Rodrigo, A.L. Worthy, Solution of multilayer diffusion problems via the Laplace transform, J. Math. Anal. Appl. 444 (1) (2016) 475–502.

[16] J. Siepmann, F. Siepmann, Modeling of diffusion controlled drug delivery, J. Control. Release 161 (2) (2012) 351–362.

[17] B. Saleh, J. Jiang, R. Fathi, T. Al-hababi, Q. Xu, L. Wang, D. Song, A. Ma, 30 years of functionally graded materials: an overview of manufacturing methods, applications and future challenges, Composites, Part B, Eng. 201 (2020) 108376.

[18] Y. Shinohara, Functionally graded materials, in: Handbook of Advanced Ceramics, second edition, 2013.

[19] A. Zimmerling, Z. Yazdanpanah, D.M.L. Cooper, J.D. Johnston, X. Chen, 3D printing PCL/nHA bone scaffolds: exploring the influence of material synthesis techniques, Biomater. Res. 25 (2021) 3.

[20] G.H. Loh, E. Pei, D. Harrison, M. Monzón, An overview of functionally graded additive manufacturing, Addit. Manuf. 23 (2018) 34–44.

[21] C. Bassand, L. Benabed, S. Charlon, J. Verin, J. Freitag, F. Siepmann, J. Soulestin, J. Siepmann, 3D printed PLGA implants: APF DDM vs. FDM, J. Control. Release 353 (2023).

[22] C. Bassand, F. Siepmann, L. Benabed, J. Verin, J. Freitag, S. Charlon, J. Soulestin, J. Siepmann, 3D printed PLGA implants: how the filling density affects drug release, J. Control. Release 363 (2023).

[23] G. Bretti, S. McGinty, G. Pontrelli, Modelling smart drug release with functionally graded materials, Comput. Biol. Med. 164 (2023).

[24] M.D. Mikhailov, General solution of the heat equation of finite regions, Int. J. Eng. Sci. 10 (1972) 577–591.

[25] M.D. Mikhailov, M.N. Özişik, Unified Analysis and Solutions of Heat and Mass Diffusion, John Wiley, New York, 1984.

[26] R.M. Cotta, C.P. Naveira-Cotta, D.C. Knupp, Nonlinear eigenvalue problem in the integral transforms solution of convection-diffusion with nonlinear boundary condition, Int. J. Numer. Methods Heat Fluid Flow 26 (2016) 767–789.

[27] C.P. Naveira-Cotta, R.M. Cotta, H.R.B. Orlande, O. Fudym, Eigenfunction expansions for transient diffusion in heterogeneous media, Int. J. Heat Mass Transf. 52 (2009) 5029–5039.

[28] R.M. Cotta, D.C. Knupp, J.N.N. Quaresma, Analytical methods in heat transfer, in: F.A. Kulacki (Ed.), Handbook of Thermal Science and Engineering, Springer, 2018, pp. 61–126.

[29] W. Szczęsna, M. Tsirigotis-Maniecka, L. Szyk-Warszyńska, S. Balicki, P. Warszyński, K.A. Wilk, Insight into multilayered alginate/chitosan microparticles for oral administration of large cranberry fruit extract, Eur. Polym. J. 160 (2021) 110776.

[30] S. Henning, D. Edelhoff, B. Ernst, S. Leick, H. Rehage, D. Suter, Characterizing permeability and stability of microcapsules for controlled drug delivery by dynamic NMR microscopy, J. Magn. Reson. 221 (2012) 11–18.

[31] D.C. Knupp, Integral transform technique for the direct identification of thermal conductivity and thermal capacity in heterogeneous media, Int. J. Heat Mass Transf. 171 (2021) 121120.